Precracked Reinforced Concrete T-Beams Repaired in Shear with Bonded Carbon Fiber-Reinforced Polymer Sheets

Dirar, Samir; Lees, J; Morley, C

This is the peer reviewed version of Dirar, S., Lees, J.M. and Morley, C.T. (2012) "Precracked RC T-beams Repaired in Shear with Externally Bonded CFRP Sheets" ACI Structural Journal v. 109, (2):215-223

PRECRACKED RC T-BEAMS REPAIRED IN SHEAR WITH BONDED CFRP SHEETS

Samir Dirar, Janet Lees and Chris Morley

Samir Dirar is a Lecturer in Structural Engineering at the University of Birmingham, United Kingdom (UK). He received his PhD in Engineering from the University of Cambridge, UK. His research interests include strengthening of existing structures with fiber reinforced polymers, nonlinear finite element analysis of concrete structures and structural health monitoring.

Janet Lees is a Senior Lecturer in Structural Engineering at Cambridge University, UK. She is interested in the use of advanced durable materials as prestressing tendons for concrete elements, strengthening and repair of existing structures, advanced numerical analyses, glass fiber reinforced polymer pipelines and sustainable concrete.

Chris Morley is a former Senior Lecturer in Concrete Structures at Cambridge University, UK. He has always been interested in plasticity theory, and especially in its application to reinforced concrete (RC) structures. His research interests extend to nonlinear finite elements analysis of RC structures, water in hardened concrete and structural analysis generally.

ABSTRACT

This paper investigates the structural behavior of precracked reinforced concrete (RC) T-beams strengthened in shear with externally bonded carbon fiber reinforced polymer (CFRP) sheets. It reports on seven tests on unstrengthened and strengthened RC T-beams identifying the influence of load history, beam depth and percentage of longitudinal steel reinforcement on the structural behavior. The experimental results indicate that the contributions of the external CFRP sheets to the shear force capacity can be significant and depend on most of the investigated variables.

This paper also investigates the accuracy of the prediction of the FRP contribution in ACI 440.2R-08; UK Concrete Society TR 55 and *fib* Bulletin 14 design guidelines for shear strengthening. Comparison of predicted values with experimental results indicates that the guidelines can overestimate the shear contribution of the externally bonded fiber reinforced polymer (FRP) system.

Keywords: beam; fiber reinforced polymer; precracking; reinforced concrete; shear; strengthening

INTRODUCTION

Throughout the world many existing reinforced concrete (RC) structures are deemed no longer able to sustain current capacity demands. In the United Kingdom (UK) alone, it has been estimated that there are about 10,000 bridges on the motorway and trunk road network (the majority of which are reinforced and prestressed concrete structures) and 150,000 bridges on local roads of which a considerable number need strengthening or replacement[1]. The estimated cost of assessing and strengthening these strength-deficient structures is in excess of £4 billion[2]. Other countries are faced by the same problem. In the United States (US) for example, of the 600,905 bridges across the country, 72,868 bridges (12.1%) were categorized as structurally deficient and 89,024 bridges (14.8%) were categorized as functionally obsolete. The estimated cost of strengthening and repairing both categories is about US$140 billion[3].

Several factors can cause a RC structure to be judged as having insufficient capacity. The need to sustain heavier loads is one important factor, particularly in the case of bridges. Further factors that can have detrimental effects on capacity include corrosion of internal steel reinforcement, changes in use, poor initial design and more stringent assessment codes.

One viable solution is to use fiber reinforced polymers (FRPs) as external strengthening reinforcement for RC structures. The use of FRPs is advantageous since the combination of high-strength, high-stiffness structural fibers with low-cost, lightweight, environmentally resistant polymers results in composite materials with excellent mechanical and durability properties.

During the past two decades, several research studies have considered RC beams strengthened in shear with externally bonded FRP systems. However, there are areas where further research is still needed. T-beams have not been considered as extensively as rectangular beams and in general studies investigating the effect of load history on the strengthened behavior have been scarce. Therefore, an attempt is made in this paper to investigate the effect of load history on the behavior of precracked RC T-beams strengthened in shear with carbon FRP (CFRP) sheets. Other parameters that may influence behavior, namely the effective depth of the beam and the longitudinal steel reinforcement ratio, are also discussed. Finally, the reliability of the prediction of the FRP shear contribution in three international shear strengthening design guidelines, namely ACI 440.2R-08[4]; UK Concrete Society TR 55[5] and *fib* Bulletin 14[6], is examined.

RESEARCH SIGNIFICANCE

Many researchers [e.g. 7-11] have investigated the technique of strengthening RC beams in shear using FRPs and established its effectiveness. Published research studies have provided valuable findings, particularly with regard to the effects of the type, stiffness and configuration of the composite material on the shear strength enhancement. However, other parameters that may also influence the shear resisting mechanisms, such as the load history, have not yet been sufficiently studied. In addition to investigating the effect of load history on the shear strength enhancement, this study simulates aspects of the in-service behavior of FRP-strengthened beams including precracking and strengthening under load.

EXPERIMENTAL INVESTIGATION

The experimental investigation consisted of two unstrengthened control beams along with five other beams that were precracked prior to the application of the CFRP sheets. All specimens were T-shaped beams having a significant difference between their unstrengthened shear capacity and their flexural capacity. The T-shaped cross-section was favored because it adequately simulates the slab-on-beam construction method. The gap between the shear capacity and the flexural capacity was deemed necessary in order to provide a sufficient range over which the level of shear enhancement could be measured.

Each specimen had a four part designation given as X/*d*/LP#/*p* where X indicates that the beam was either unstrengthened (U) or strengthened with CFRP fabrics (F), *d* is the effective depth of the beam in mm, LP# indicates the loading pattern to which the beam was subjected and *p* indicates the longitudinal reinforcement ratio ($A_s/b_w d$) of the beam. Hence, the designation F/295/LP1/4.5 refers to a beam that was strengthened with CFRP fabrics (sheets), had an effective depth of 295 mm (11.61 in.), tested under loading pattern 1 (LP1) and had a longitudinal reinforcement ratio of 4.5%.

All tested shear spans had 6 mm (0.24 in.) internal steel transverse reinforcement spaced at 250 mm (9.84 in.) c/c. For the strengthened beams, the external shear reinforcement on a strengthened shear span consisted of three layers of CFRP sheets.

The two T-shaped cross-sections considered in this experimental investigation are detailed in **Fig. 1**. Additional details of the test specimens are given in **Table 1**.

Loading patterns

Three loading schemes were adopted for testing. Loading Pattern 0 (LP0), which was only applied to test the control specimen U/295/LP0/4.5, consisted of loading the beam up to

failure. The remaining two loading patterns, namely Loading Pattern 1 (LP1) and Loading Pattern 2 (LP2), involved the pre-cracking of the test specimens in order to model the state of damage that may exist in RC structures requiring strengthening. Tests on the unstrengthened beams showed that the state of damage caused by a load level of about 70% of the unstrengthened shear force capacity can be representative of the state of damage that may exist in some RC structures requiring strengthening. Hence, that load level was used in both LP1 and LP2 described below. Since RC structures may also be carrying dead loads while being strengthened, specimens were unloaded to a proportion of the unstrengthened capacity before the CFRP strengthening system was applied. The final phase involved loading the strengthened specimens up to failure.

Specimens subjected to LP1 were loaded, as shown in **Fig. 2**, to 70% of the unstrengthened capacity of the corresponding control beam. Specimens were then unloaded to 40% of the unstrengthened capacity of the corresponding control beam and the strengthening system was installed. Loading then continued up to failure. Under this loading pattern, the shear cracks formed prior to strengthening are likely to be mobilized once strengthened.

LP2 aims to stimulate a set of shear cracks after strengthening that are different from those formed prior to strengthening. Specimens subjected to LP2 were initially loaded at position (B), as illustrated in **Fig. 2**, to 70% of their unstrengthened capacity. Specimens were then unloaded to 40% of their unstrengthened capacity and the strengthening system was installed. Load was then shifted gradually to position (A) and continued up to the failure of the specimens. The total load was kept constant at 40% of the unstrengthened capacity of the test beam as it was shifted from position (B) to position (A).

Test setup

All the beams except U/295/LP2/4.5 and F/295/LP2/4.5 represented a single specimen tested in four-point bending (see **Fig. 3**). However, in order to speed up the final stages of the testing process, U/295/LP2/4.5 and F/295/LP2/4.5 were tested in three-point bending as this type of loading allowed two tests to be carried out on a single beam. This was achieved by testing one beam end zone while keeping the other end overhung and unstressed and vice versa (see **Fig. 3**). The 925 mm (36.42 in.) long shear span was reinforced with additional transverse steel reinforcement (6 mm [0.24 in.] shear links spaced at 100 mm [3.94 in.] c/c) to ensure that failure always occurred in the 1125 mm (44.29 in.) long shear span. The shear span to effective depth ratio (*a/d*) in all beams was maintained at a value of 3.8.

Materials

The concrete used to cast the specimens consisted of coarse gravel aggregate (10 mm [0.39 in.] maximum size), fine aggregate (sand) and ordinary Portland cement (ASTM C150 Type I). The mix proportions by weight were cement : sand : gravel = 1 : 2.75 : 3.36. The water/cement ratio was 0.7. The targeted cube compressive strength after 28 days was 25 MPa (3.63 ksi). This value was favored because it simulates the deterioration in the concrete compressive strength that may exist in deficient RC structures.

Tensile tests were carried out on the steel reinforcement used in this study in order to quantify its mechanical properties. The test results for the strength and stiffness properties of the steel reinforcement are given in **Table 2**.

The CFRP fabrics (sheets) used in this investigation were the commercially available SikaWrap-230C. These are unidirectional woven carbon fiber fabrics that are usually used in conjunction with an epoxy laminating resin, in this case Sikadur-330, to provide a composite strengthening system. The fabric, adhesive and laminate (i.e. fabric + adhesive) properties, as obtained from the manufacturer's data sheets[12,13], are presented in **Table 3**.

Instrumentation

The deflections of all specimens were measured with linear resistance displacement transducers (LRDTs). The LRDTs were positioned either at mid-span for the beams tested in four-point bending or at position (A), i.e. at $a = 3.8d$ (see **Fig. 2**), for the specimens tested in three-point bending.

The strain in the transverse steel reinforcement and in the CFRP sheets was measured with strain gauges. The strain gauges were bonded to the internal steel reinforcement before casting whereas the strain gauges on the CFRP sheets were bonded to the surface of the sheet after it had cured but before starting the final phases of LP1 and LP2. **Fig. 3** illustrates the locations of these strain gauges. The strain gauges on the transverse steel reinforcement are designated TR# where # indicates the strain gauge number. Similarly, CF# indicates the strain gauge number for the strain gauges on the CFRP sheets. Strain gauges on the steel and CFRP shear reinforcement are spaced 250 mm (9.84 in.) c/c.

The LRDTs and strain gauge readings were acquired using an automatic data logging system.

EXPERIMENTAL RESULTS AND DISCUSSION

Shear force capacity

The unstrengthened shear capacity of each specimen as well as the shear force at failure and the gain in shear capacity above the corresponding unstrengthened control beam are presented in **Table 4**. The unstrengthened control beam tested by Hoult and Lees[14] is nominally identical to F/215/LP1/4.6 and F/215/LP2/4.6. Hence, it will be used as a basis of comparison for these two beams. It failed in shear at a shear force of approximately 88 kN (19.78 kips).

Specimen U/295/LP0/4.5 was an unstrengthened control beam designed to fail in shear in order to create a baseline reading for the 350 mm (13.78 in.) deep specimens. The unstrengthened specimen U/295/LP2/4.5 was tested to examine the effect of LP2 on the shear carrying capacity of an unstrengthened beam.

The shear force carried by U/295/LP0/4.5 at failure was 107 kN (24.05 kips). The other unstrengthened specimen, i.e. U/295/LP2/4.5, attained a shear force of 116 kN (26.08 kips) at failure. The difference in shear force capacity between the two specimens was approximately 8%, suggesting that using LP2 had little significant effect on the shear force capacity of U/295/LP2/4.5.

The 350 mm (13.78 in.) deep strengthened specimens F/295/LP1/4.5 and F/295/LP2/4.5 failed at a shear force of 135 kN (30.35 kips) and 133.5 kN (30.01 kN) respectively, attaining increases in shear force capacity of 26.2% and 24.8% respectively. The corresponding 270 mm (10.63 in.) deep strengthened specimens (F/215/LP1/4.6 and F/215/LP2/4.6) failed at a shear force of 102.5 kN (23.04 kips) and 96.5 kN (21.69 kips) respectively, achieving increases of 16.5% and 9.7% respectively.

Specimen F/295/LP1/3.3 attained a shear force of 122.5 kN (27.54 kips) at failure corresponding to 14.5% shear enhancement. This specimen failed in flexure. Although not reported in detail in this paper, the readings of strain gauges on the longitudinal steel of F/295/LP1/3.3 showed clearly that yielding had occurred. Due to the flexural failure of F/295/LP1/3.3, it is possible that the difference in the shear carrying capacities between F/295/LP1/3.3 and F/295/LP1/4.5 is a consequence of specimen F/295/LP1/3.3 attaining its flexural capacity rather than a consequence of the change in the longitudinal reinforcement ratio. Hence, it can only be concluded that the capacity of F/295/LP1/3.3 was increased by at least 15.5 kN (3.49 kips).

The two load histories investigated, LP1 and LP2, did not generally seem to have a significant effect on the load carrying capacity of the strengthened beams. There was less than a 7% capacity difference in the 270 mm (10.63 in.) deep strengthened beams and the 350 mm (13.78 in.) deep strengthened beams did not show any significant difference in capacity.

During testing, it was clear that pre-existing cracks were interacting with subsequent crack formation yet interestingly this interaction did not seem to impact greatly on the peak load at failure. As will be explained later in this paper, the strengthened beams failed due to the debonding of the CFRP sheets. Such debonding failures could conceal any possible load effects that may have affected the shear force capacity at a further loading stage. This possibility may be further investigated by preventing debonding at a fairly early stage. This can be achieved either by fully wrapping the beam or, more practically, by using fasteners to secure the CFRP sheets and so exploit its tensile strength more effectively.

The CFRP contribution of the strengthened beams was clearly affected by the change in beam depth. It increased with increasing depth from 14.5 kN (3.26 kips) to 28 kN (6.30 kips) in the strengthened beams subjected to LP1 and from 8.5 kN (1.91 kips) to 26.5 kN (5.96 kips) in the strengthened beams subjected to LP2. These results suggest that the bonded fabric system is more effective when used on the "deeper" 350 mm (13.78 in.) beams. In the "shallower" 270 mm (10.63 in.) deep specimens, the fabric strengthening was not fully effective since only a fairly short bonded length is available for force transfer. Another explanation could be that the "deeper" beams had more CFRP area bridging a shear crack compared to the "shallower" beams.

Shear force-deflection relationship

The shear force-deflection curves for the specimens considered in this investigation are presented in **Fig. 4**. Except for F/295/LP1/3.3 which failed in flexure, all specimens experienced a drop in load at peak shear force which is a characteristic of brittle (shear) failure. The unstrengthened specimens were more brittle compared to the corresponding strengthened specimens. The deflection ratio between the strengthened beams that failed in shear and the corresponding unstrengthened beams, however, is of the same order of magnitude, approximately 1.22.

In the initial loading stage (up to 70% of the unstrengthened capacity), the strengthened beams, except F/215/LP2/4.6 as it was initially loaded at a shorter shear span, behaved similarly to the corresponding unstrengthened specimens.

In the final loading stage, all the strengthened beams attained slightly higher stiffness, which deteriorated gradually with increased loading due to cracking until failure occurred. Specimens U/295/LP2/4.5 and F/295/LP2/4.5 show stiffer shear force-deflection relationships as they had shorter lengths.

Specimen F/295/LP1/3.3 had the same geometrical dimensions as the other 350 mm (13.78 in.) deep specimens. However, its longitudinal steel ratio was 27% less. That is why, after the initial flexural cracking of the concrete at a shear force of about 20 kN (4.5 kips), this beam experienced more deflection at a given shear force compared to U/295/LP1/4.5 and F/295/LP1/4.5. This difference in deflection at the end of the pre-cracking process was in excess of 2mm (0.08 in.). Except for the extra deflection, at reloading the behavior of F/295/LP1/3.3 was similar to that of F/295/LP1/4.5 up to a shear force of 122.5 kN (27.54 kips). At that load level, the beam developed ductile behavior as illustrated by the approximately 10 mm (0.39 in.) long yield plateau seen in **Fig. 4** and then failed in flexure.

Failure mode

The two unstrengthened beams failed in shear as shown in **Fig. 5**. U/295/LP0/4.5 failed due to an inclined crack that ran from the support to the load point. This inclined crack followed a path at an angle of approximately 24° in the web and a much shallower path in the flange.

Specimen U/295/LP2/4.5 failed due to an inclined crack that penetrated the flange and propagated towards the load pad. This was accompanied by the excessive opening of one of the inclined cracks in the web as shown in **Fig. 5**. Of importance is that the inclined shear crack that formed in the first stage of loading remained stable and did not contribute to the failure mechanism. This may explain why load case LP2 had little effect on the shear carrying capacity.

Specimens F/295/LP1/4.5 and F/295/LP2/4.5 failed due to an inclined crack that extended into the flange and ran to the load pad. This was preceded by the debonding of the CFRP sheets located between the splitting zones shown in **Fig. 6** and the load pads. The fabric splitting was caused by a set of vertical cracks that formed initially in the flange and extended downward to the web. The formation of such cracks in the flange can be explained by strain compatibility between the flange and the web. With increased loading, the web portion between the support and the major shear crack attempts to rotate. However, the flange restrains its movement. Consequently, horizontal tensile strains and stresses develop in the top part of the flange. Eventually, the tensile stresses exceed the tensile strength of the concrete and vertical cracks form. Hence, the fabric splitting close to the support region of the beam may be prevented by applying a layer of the unidirectional CFRP sheets parallel to the longitudinal axis of the beam.

Specimen F/215/LP2/4.6, which was tested before F/215/LP1/4.6, is pictured at failure in **Fig. 7**. Initially, the fabrics started to peel off at the web-flange interface closer to the support. The beam failed due to peeling off of the fabrics and concrete failure in the end region of the beam before the inclined cracks could reach the load pad. However, the penetration of the inclined cracks well into the flange and their progress toward the load pad were signs that shear failure was imminent. It is possible that the reduced support area in this specimen due to chamfering and the relatively short overhang might have led to concrete failure in the end region of the beam.

When the support area was not chamfered and the overhang length was increased in specimen F/215/LP1/4.6, the beam failed in shear as shown in **Fig. 7**. The fabrics started to peel off in a similar way to that of F/215/LP2/4.6 and the inclined cracks continued to propagate towards the load pad and backwards above the support and into the overhang until, eventually, they led to beam failure. This was accompanied by separation between concrete and fabrics as can also be seen in **Fig. 7**.

Specimen F/295/LP1/3.3 failed in flexure due to the crushing of the concrete in the compression zone at the middle of the beam as shown in **Fig. 8**. This result is important as it shows that the externally bonded CFRP sheets can change the mode of failure from a brittle shear failure to a ductile flexural failure. The CFRP composites in the two shear spans of F/295/LP1/3.3 were still intact and bonded to the beam web at failure.

It was not possible to measure the width of shear cracks in the strengthened specimens as these cracks were covered by the CFRP sheets. Nevertheless, It was expected that very limited size effects, if any, existed due to the limited increase in beam depth from 270 mm (10.63 in.) to 350 mm (13.78 in.).

Strain in the steel shear reinforcement

This section reports on the strain in the transverse steel reinforcement in the shear spans where failure occurred. **Fig. 3** shows the positions of the strain gauges on the transverse steel reinforcement. For the purpose of interpreting results, the shear links are categorized into "outer links" (TR1), "middle links" (TR2 and TR3 in the 350 mm [13.78 in.] deep specimens, and TR2 in the 270 mm [10.63 in.] deep specimens) and "inner links" (TR4 in the 350 mm [13.78 in.] deep specimens and TR3 in the 270 mm [10.63 in.] deep specimens). Unfortunately, some strain gauges failed during testing and their results were discarded.

The outer and middle shear links in the unstrengthened beams started to function only after a shear force of between 30 kN (6.74 kips) and 45 kN (10.12 kips) (see **Fig. 9**). Thereafter, the

strain in the stirrups increased significantly with increasing load. Most of the shear links in this group attained their yield strain after a shear force of approximately 90 kN (20.23 kips). This was expected since these links were crossed by the major shear cracks.

The outer and middle shear links in the strengthened beams experienced five phases during loading. In the initial phase, which is bounded on the upper end by a shear force between 35 kN (7.87 kips) and 45 kN (10.12 kips), the contribution of the shear links to the resistance was negligible. In the second phase, which included loading to 70% of the unstrengthened shear capacity, the shear links started to develop strain due to the initiation and propagation of inclined cracks. In the third phase, unloading to 40% of the unstrengthened shear capacity reduced the strain in the outer and middle shear links. The fourth phase is marked by the addition of the CFRP sheets and the stiffer response shown by the transverse steel reinforcement on further reloading. The transverse steel strain showed limited increases with increasing load until, in the final stage, yielding was achieved in most cases. The transverse steel reinforcement that yielded is easily identified by the plateaus featured in **Fig. 9**.

Fig. 9 also shows that the inner links carried the least amount of strain in all test specimens. The strains in this group of transverse reinforcement developed at a relatively low rate even after the formation of shear cracks. This is mainly because the beam region close to the load pad, where the inner links were located, did not experience significant inclined cracking.

Strain in the CFRP sheets

The shear force-strain curves for the externally bonded CFRP sheets in the shear spans where failure occurred are shown in **Fig. 9**. The positions of the strain gauges are given in **Fig. 3**. The fabrics are categorized into “outer fabrics” (CF1), “middle fabrics” (CF2 and CF3 in the 350 mm [13.78 in.] deep specimens, and CF2 in the 270 mm [10.63 in.] deep specimens) and “inner fabrics” (CF4 in the 350 mm [13.78 in.] deep specimens and CF3 in the 270 mm [10.63 in.] deep specimens). Some strain gauges failed during testing and their results were discarded due to the erroneous data they provided.

The curves feature two phases. In the first phase, the fabrics started to resist the further opening of existing shear cracks at the inception of the final reloading stage. They continued to develop tensile strain with increased load up to approximately the peak loads. In the second stage, the fabrics started to debond and finally peeled off. Debonding is indicated by the reversing of the shear force-strain curves.

In a given beam, the middle fabrics – represented by CF3 in the 350 mm (13.78 in.) deep specimens and CF2 in the 270 mm (10.63 in.) deep specimens – developed the highest strain.

The sheets bonded to the 350 mm (13.78 in.) deep specimens developed higher strains compared to those bonded to the 270 mm (10.63 in.) deep specimens. This increase in the effectiveness of the fabrics can be explained by the increase in bond length. This result highlights the fact that the deeper the section, the higher the potential of the sheets to experience strain and hence provide shear enhancement.

COMPARISON OF EXPERIMENTAL RESULTS WITH PREDICTIONS OF SHEAR STRENGTHENING DESIGN GUIDELINES

Design guidelines for externally bonded FRP shear reinforcement have been developed in the UK and elsewhere. In the UK, the Concrete Society Technical Report 55[5] (TR 55) is the first – and currently the sole – standard document to give guidance on the design of externally bonded FRP shear reinforcement. The design procedure adopted by TR 55[5] is based upon that proposed by Denton et al.[15] and assumes that the ultimate shear capacity of an FRP strengthened beam can be expressed as the sum of the shear forces carried by the concrete, the internal steel shear reinforcement and the external FRP shear reinforcement. Similarly, the ACI 440.2R-08[4] shear strengthening design model, based on work by Khalifa et al.[16], and *fib* Bulletin 14[6] shear strengthening design guidelines, based on work by Triantafillou and Antonopoulos[17], use the same approach as TR55[5], assuming that the shear capacity of a strengthened RC beam can be expressed as the sum of the concrete, steel and FRP contributions. Further, the FRP contribution in the three aforementioned design guidelines is determined by adopting the truss analogy and assuming the inclination angle of the shear cracks to be 45°. The main difference among the three models is in the method of evaluating the effective strain in the FRP reinforcement.

A database of eight experimental results against which to compare the predictions of ACI 440.2R-08[4], TR55[5] and *fib* Bulletin 14[6] has been assembled. The database beams had T-shaped cross-sections, internal steel shear reinforcement, and shear span to effective depth ratios greater than or equal to 2.5. Although the design guidelines should be validated with a larger database, there have not been so many tests on RC Beams that meet the above criteria. RC beams that do not meet the above criteria are deemed to lie beyond the scope of this study and hence are not included in the database.

Three of the database beams are the fabric-strengthened beams F/295/LP1/4.5, F/295/LP2/4.5, and F/215/LP1/4.6 detailed in this study. The other five beams are SB-S1-2L-175 and SB-S1-0.5L-350 tested by Bousselham and Chaallal[7,8], Specimen No. 2 tested by Sato et al.[18], and T4S2-C45 and T6S4-C90 tested by Deniaud and Cheng[19,20]. All beams included in the

database, except those tested by Deniaud and Cheng[19,20], were strengthened with continuous U-shaped externally bonded CFRP shear reinforcement. The externally bonded shear reinforcement in the beams tested by Deniaud and Cheng[19,20] consisted of CFRP U-strips spaced 100 mm (3.94 in.) c/c. All beams included in the database failed in shear due to the peeling off of the CFRP reinforcement.

Table 5 compares the contributions of the externally bonded CFRP system predicted by the ACI 440.2R-08[4], TR55[5] and *fib* Bulletin 14[6] design guidelines with the experimental results from the literature and the testing described in this paper. All safety factors are set equal to 1.00 for the purpose of the comparison except for the ACI 440.2R-08[4] FRP strength reduction factor, ψ_f, which is set equal to 0.85 as it is an integral part of the nominal shear capacity expression. The experimental contributions of the CFRP sheets were calculated by subtracting the experimental unstrengthened shear capacity from the experimental strengthened shear capacity for each beam. It should be noted that some of the strengthened beams reported in this paper had slightly higher concrete compressive strength than the corresponding unstrengthened beams. However, further analyses carried out by the authors (not reported in this paper) showed that this slight difference in the concrete compressive strength had little significant effect on the predicted FRP contribution.

The total predicted shear force has not been compared to the total experimental shear force because such a comparison can lead to erroneous conclusions. Such a comparison requires the use of conventional design codes such as the Eurocode 2[21] (EC 2) to calculate the concrete and steel contributions to the total shear force capacity. Such codes often underestimate the concrete and steel contributions to the total shear force because they assume that only the web of the beam is effective when calculating the shear force capacity of a T-beam. For example, the total predicted shear force capacity of F/215/LP1/4.6 using the EC 2[21] and the TR 55[5] design equations is 94.1 kN (21.15 kips). As the total experimental shear capacity of F/215/LP1/4.6 is 102.5 kN (23.04 kips), this would lead to the conclusion that the design model of the TR 55[5] which overestimates the FRP contribution to the shear force capacity of F/215/LP1/4.6 by a factor of 2.08, is safe. Hence, while comparing the total experimental shear force capacity to the total predicted shear force capacity could result in a conservative prediction; such a comparison may lead to the erroneous conclusion that an over-conservative CFRP design model is safe.

The ACI 440.2R-08[4] design model is statistically the best model among the three design models investigated. However, the ACI 440.2R-08[4] design model has a mean predicted to experimental ratio of 1.41 and a standard deviation of 0.53. This is probably due to the fact

that the bond model used in the ACI 440.2R-08[4] design model is based on limited experimental data.

The TR 55[5] predictions overestimated the contributions of the externally bonded CFRP sheets to the shear force capacity with a mean predicted to experimental ratio of 1.64 and a standard deviation of 0.62. The inaccuracy of the TR 55[5] predictions stems from the inaccuracy of its effective strain model. TR55[5] predicts that the effective strain in the CFRP sheets of F/295/LP1/4.5, F/295/LP2/4.5 and F/215/LP1/4.5 is approximately 2560 micro-strain, 2650 micro-strain and 2810 micro-strain respectively. The experimentally measured CFRP strain for these beams varied between 125 micro-strain and 1200 micro-strain (see **Fig. 9**).

The *fib* Bulletin 14[6] design model is statistically the worst model among the three design models investigated. It has a mean predicted to experimental ratio of 2.52 and a standard deviation of 0.76. The deficiency of the model is probably due to the fact that the equations for the effective FRP strain were obtained by regression analysis with limited experimental data. Hence, the effective FRP strain equations do not consider the bond mechanism which affects the mode of failure.

SUMMARY AND CONCLUSIONS

This study investigates the structural behavior of precracked RC T-beams strengthened in shear with externally bonded CFRP sheets. The influence of load history, effective depth of the beam and longitudinal steel ratio on the strengthened behavior was studied. The predictions of three international shear strengthening design guidelines were compared with experimental results. Based on the results of this study, the following conclusions are drawn:

1. All strengthened specimens exhibited greater capacities than equivalent unstrengthened control beams, with capacity enhancements ranging from 9.7% to 26.2%, confirming the potential effectiveness of the CFRP sheets.
2. The two loading patterns investigated, LP1 and LP2, did not generally seem to have a significant effect on the shear capacity of the strengthened beams. During testing it was clear that pre-existing cracks were interacting with subsequent crack formations yet this interaction did not seem to impact greatly on the peak load at failure.
3. The increase in beam depth positively affected the contribution of the CFRP sheets to the shear force capacity through providing additional bond length to better exploit the sheets' tensile strength.
4. The decrease in the longitudinal reinforcement ratio from 4.5% to 3.3% changed the mode of failure from brittle shear failure to ductile flexural failure.

5. The ACI 440.2R-08[4], TR55[5] and *fib* Bulletin 14[6] shear strengthening design guidelines overestimated the contribution of the externally bonded CFRP sheets with mean predicted to experimental ratios of 1.41, 1.64, and 2.52, and standard deviations of 0.53, 0.62, and 0.76 respectively.

ACKNOWLEDGMENTS

The financial support of the UK Engineering and Physical Sciences Research Council (EPSRC) through grant GR/S55101/01 is gratefully acknowledged.

NOTATION:

A_s = area of steel tension reinforcement

a = shear span

b_w = web width

d = effective beam depth

f_{cu} = cube compressive strength

p = longitudinal reinforcement ratio

ψ_f = FRP strength reduction factor used in the nominal shear capacity expression suggested by the ACI 440.2R-08

REFERENCES

1. Middleton, C. R., "Bridge Management and Assessment in the UK," *Proceedings of Austroads 5th Bridge Conference*, Austroads, Australia, 2004, 16pp.

2. Middleton, C. R., "Concrete Bridge Assessment: An Alternative Approach," *The Structural Engineer*, The Institution of Structural Engineers, United Kingdom, V. 75, No. 23/24, 1997, pp. 403-409.

3. ASCE Advisory Council, "2009 Report Card for America's Infrastructure," American Society of Civil Engineers (ASCE), Reston, Virginia, 2009, 153 pp.

4. ACI Committee 440, "Guide for the Design and Construction of Externally Bonded FRP Systems for Strengthening Concrete Structures (440.2R-08)," American Concrete Institute (ACI), Farmington Hills, Mich., 2008, 76 pp.

5. The Concrete Society, "Technical Report 55 (TR55): Design Guidance for Strengthening Concrete Structures using Fibre Composite Materials," Crowthorne, United Kingdom, 2004, 72 pp.

6. *fib* Task Group 9.3, "Bulletin 14: Externally Bonded FRP Reinforcement for RC Structures," International Federation for Structural Concrete (*fib*), Lausanne, Switzerland, 2001, 138 pp.

7. Bousselham, A., and Chaallal, O., "Effect of Transverse Steel and Shear Span on the Performance of RC Beams Strengthened in Shear with CFRP," *Composites Part B: Engineering*, Elsevier, The Netherlands, V. 37, No. 1, 2006, pp. 37-46.

8. Bousselham, A., and Chaallal, O., "Behaviour of Reinforced Concrete T-Beams Strengthened in Shear with Carbon Fiber-Reinforced Polymer – An Experimental Study," *ACI Structural Journal*, V. 103, No. 3, 2006, pp. 339-347.

9. Khalifa, A., and Nanni, A., "Rehabilitation of Rectangular Simply Supported RC Beams with Shear Deficiencies Using CFRP Composites," *Construction and Building Materials*, Elsevier, The Netherlands, V. 16, No. 3, 2002, pp. 135-146.

10. Pellegrino, C., and Modena, C., "Fiber Reinforced Polymer Shear Strengthening of Reinforced Concrete Beams with Transverse Steel Reinforcement," *ASCE Journal of Composites for Construction*, V. 6, No. 2, 2002, pp. 104-111.

11. Chaallal, O., Shahawy, M., and Hassan, M., "Performance of Reinforced Concrete T-Girders Strengthened in Shear with Carbon Fiber-Reinforced Polymer Fabrics," *ACI Structural Journal*, V. 99, No. 3, 2002, pp. 335-343.

12. Sika Limited, "SikaWrap-230C Product Data Sheet," United Kingdom, 2005, 4pp.

13. Sika Limited, "Sikadur-330 Product Data Sheet," United Kingdom, 2005, 6pp.

14. Hoult, N. A., and Lees, J. M., "Efficient CFRP Strap Configurations for the Shear Strengthening of Reinforced Concrete T-Beams," *ASCE Journal of Composites for Construction*, V. 13, No. 1, 2009, pp. 45-52.

15. Denton, S. R., Shave, J. D., and Porter, A. D., "Shear Strengthening of Reinforced Concrete Structures Using FRP Composites," *Proceedings of the 2nd International Conference on Advanced Polymer Composites for Structural Applications in Construction (ACIC 2004)*, Woodhead Publishing Ltd., United Kingdom, 2004, pp. 134-143.

16. Khalifa, A., Gold, W. J., Nanni, A., and Aziz, A. M. I., "Contribution of Externally Bonded FRP to Shear Capacity of RC Flexural Members," *ASCE Journal of Composites for Construction*, V. 2, No. 4, 1998, pp. 195-202.

17. Triantafillou, T. C., and Antonopoulos, C. P., "Design of Concrete Flexural Members Strengthened in Shear with FRP," *ASCE Journal of Composites for Construction*, V. 4, No. 4, 2000, pp. 198-205.

18. Sato, Y., Ueda, T., Kakuta, Y., and Ono, S., "Ultimate Shear Capacity of Reinforced Concrete Beams with Carbon Fiber Sheet," *Proceedings of the 3rd International Symposium on Non-Metallic (FRP) Reinforcement for Concrete Structures*, Japan Concrete Institute, Japan, V. 1, 1997, pp. 499-506.

19. Deniaud, C., and Cheng, J. J. R., "Reinforced Concrete T-Beams Strengthened in Shear with Fiber Reinforced Polymer Sheets," *ASCE Journal of Composites for Construction*, V. 7, No. 4, 2003, pp. 302-310.

20. Deniaud, C., and Cheng, J. J. R., "Shear Behavior of Reinforced Concrete T-Beams with Externally Bonded Fiber-Reinforced Polymer Sheets," *ACI Structural Journal*, V. 98, No. 3, 2001, pp. 386-394.

21. British Standards Institution, "Eurocode 2: Design of Concrete Structures – Part 1-1: General Rules and Rules for Buildings," London, England, 2004, 225pp.

Table 1–Summary of test specimens

Specimen	f_{cu}, MPa (ksi)	a, mm (in.)	d, mm (in.)	A_s, mm^2 (in.^{2})
U/295/LP 0/4.5	24 (3.48)	1125 (44.29)	295 (11.61)	1383 (2.14)
U/295/LP 2/4.5	28 (4.06)	1125 (44.29)	295 (11.61)	1383 (2.14)
F/295/LP 1/4.5	24 (3.48)	1125 (44.29)	295 (11.61)	1383 (2.14)
F/295/LP 2/4.5	27 (3.92)	1125 (44.29)	295 (11.61)	1383 (2.14)
F/295/LP 1/3.3	28 (4.06)	1125 (44.29)	295 (11.61)	1030 (1.60)
F/215/LP 1/4.6	32 (4.64)	820 (32.28)	215 (8.46)	1030 (1.60)
F/215/LP 2/4.6	25 (3.63)	820 (32.28)	215 (8.46)	1030 (1.60)

Table 2–Steel reinforcement properties

Bar diameter, mm (in.)	Yield strength, MPa (ksi)	Yield strain	Ultimate strength, MPa (ksi)
6 (0.24)	580 (84.12)*	0.0050*	586 (84.99)
8 (0.31)	520 (75.42)	0.0028	594 (86.15)
16 (0.63)	500 (72.52)	0.0032	593 (86.01)
20 (0.79)	580 (84.12)	0.0038	680 (98.63)
25 (0.98)	440 (63.82)*	0.0044*	540 (78.32)

* Using the 0.2% offset method.

Table 3–CFRP sheets and adhesive properties

Material	Tensile strength, MPa (ksi)	Ultimate strain	Elastic modulus, MPa (ksi)
CFRP sheets*	4300 (623.66)	0.0180	238000 (34519)
Epoxy resin	30 (4.35)	0.0090	4500 (653)
Composite material**	350 (50.76)	0.0125	28000 (4061)

* Nominal thickness per layer = 0.131 mm (0.0052 in.).

** Nominal thickness per layer = 1 mm (0.0394 in.).

Table 4–Experimental results

Specimen	Unstrengthened shear capacity, kN (kips)	Shear force at failure, kN (kips)	Gain in shear strength, kN (kips)	Gain in shear strength, %
U/295/LP0/4.5	107.0 (24.05)	107.0 (24.05)	0 (0)	0
U/295/LP2/4.5	107.0* (24.05)	116.0 (26.08)	9 (2.03)	8.4
F/295/LP1/4.5	107.0 (24.05)	135.0 (30.35)	28.0 (6.30)	26.2
F/295/LP2/4.5	107.0 (24.05)	133.5 (30.01)	26.5 (5.96)	24.8
F/295/LP1/3.3	107.0 (24.05)	122.5 (27.54)	15.5 (3.49)	14.5
F/215/LP1/4.6	88.0** (19.78)	102.5 (23.04)	14.5 (3.26)	16.5
F/215/LP2/4.6	88.0** (19.78)	96.5 (21.69)	8.5 (1.91)	9.7

* For purpose of comparison with U/295/LP0/4.5.

** Based on the control beam, tested by Hoult and Lees[14], which is nominally identical to F/215/LP1/4.6 and F/215/LP2/4.6.

Table 5–Experimental versus predicted shear resistance due to FRPs

Specimen	Experimental, kN (kips)	ACI 440.2R-08[4], kN (kips)	TR55[5], kN (kips)	*fib* Bulletin 14[6], kN (kips)
F/295/LP1/4.5	28.0 (6.30)	51.4 (11.56)	63.1 (14.19)	70.1 (15.76)
F/295/LP2/4.5	26.5 (5.96)	56.7 (12.74)	66.7 (14.99)	74.1 (16.66)
F/215/LP1/4.6	14.5 (3.26)	31.6 (7.11)	30.1 (6.77)	57.5 (12.93)
SB-S1-2L-175[7]	12.2 (2.74)	14.9 (3.34)	21.8 (4.90)	26.6 (5.98)
SB-S1-0.5L-350[8]	19.2 (4.32)	23.5 (5.30)	23.0 (5.17)	49.0 (11.02)
Specimen No. 2[18]	24.0 (5.40)	21.8 (4.90)	23.9 (5.37)	50.2 (11.29)
T4S2-C45[19]	17.8 (4.00)	19.2 (4.32)	30.2 (6.79)	52.2 (11.74)
T6S4-C90[20]	85.3 (19.18)	61.0 (13.72)	50.2 (11.29)	95.8 (21.54)

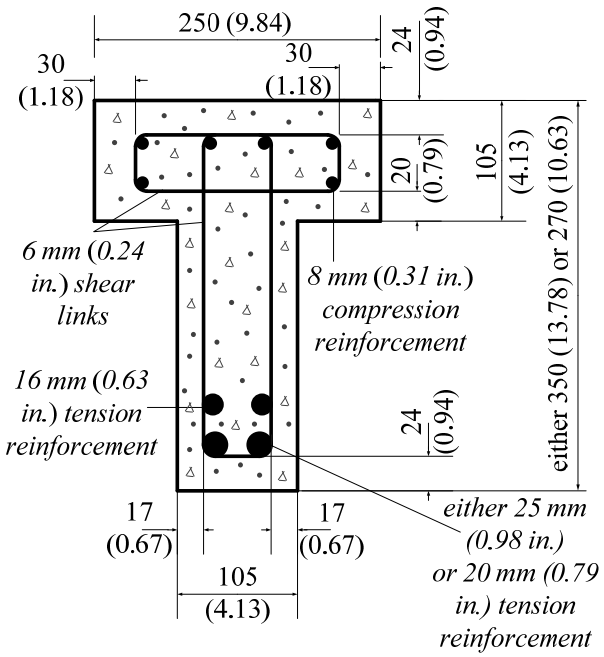

Fig. 1– Cross-sections details – dimensions in mm (in.).

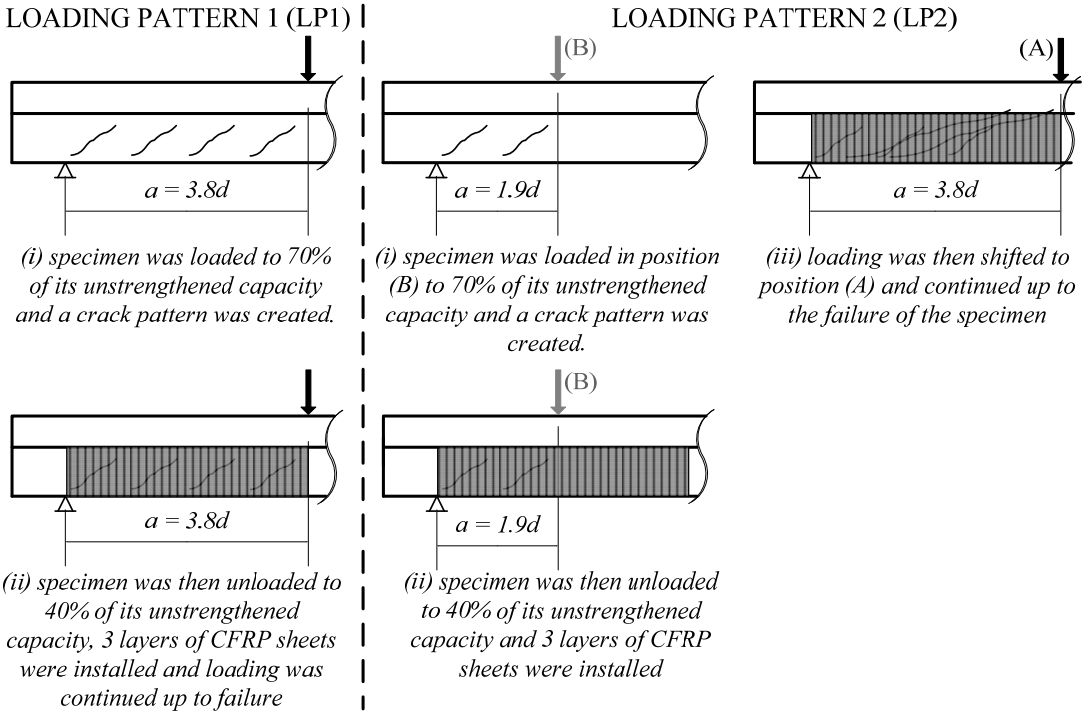

Fig. 2–Loading patterns.

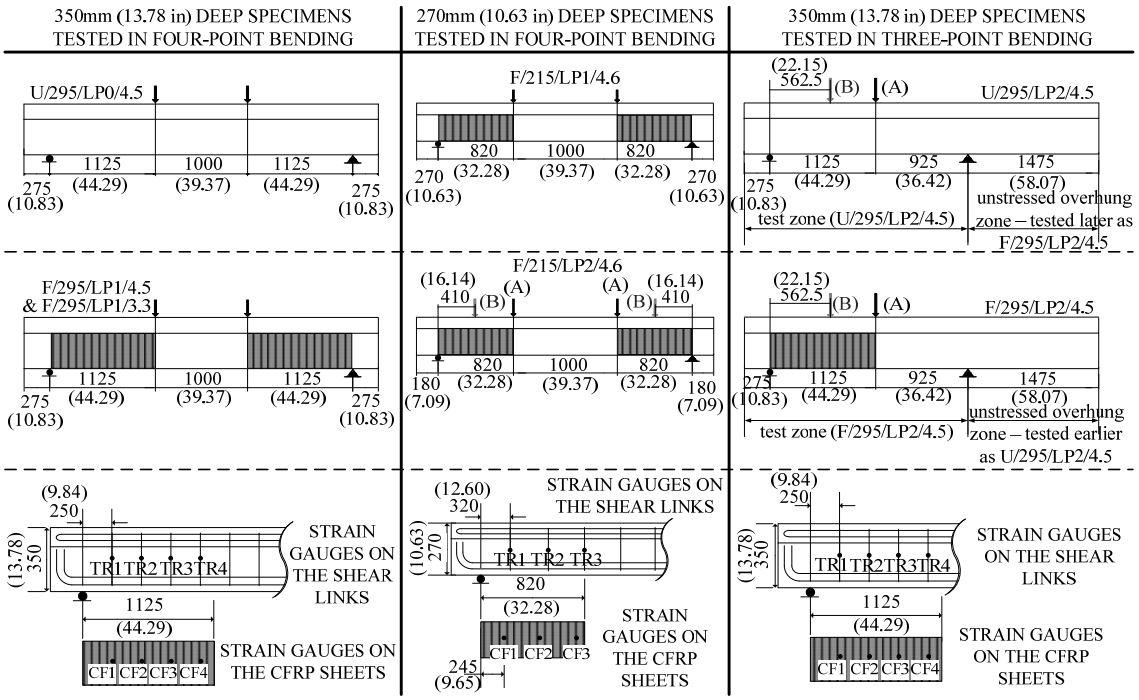

Fig. 3– Details of test specimens – dimensions in mm (in.).

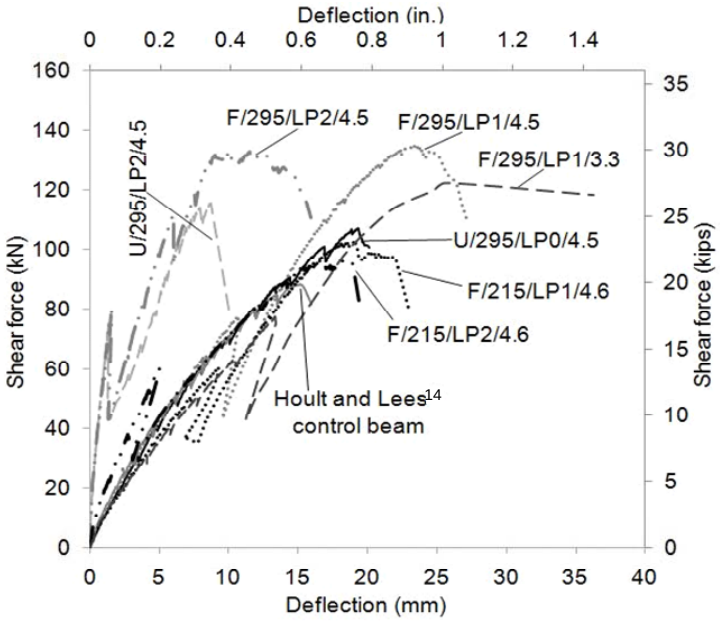

Fig. 4–Shear force-deflection curves.

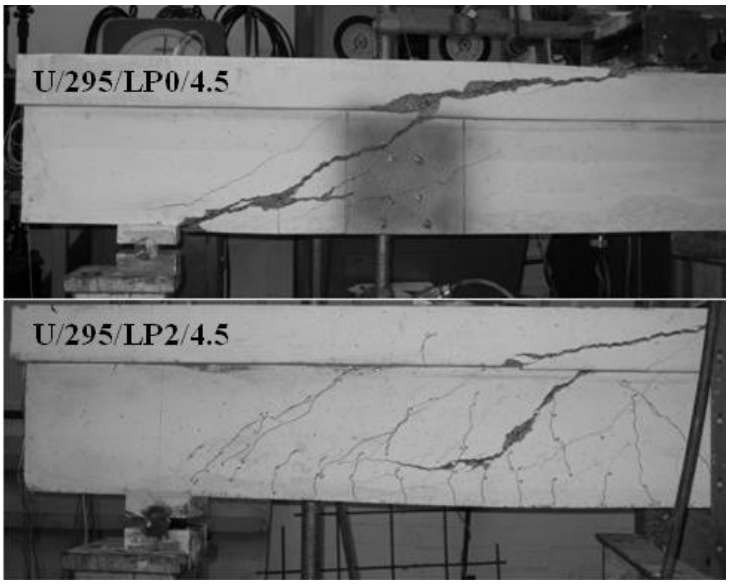

Fig. 5–Unstrengthened specimens at failure.

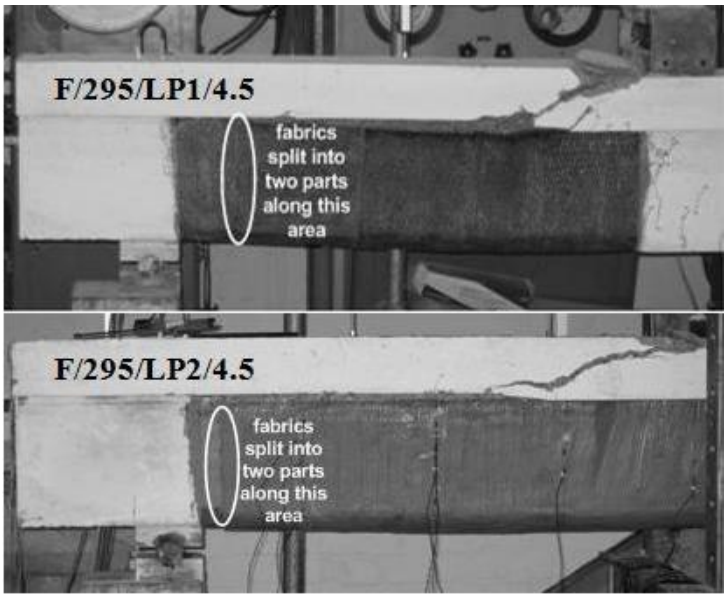

Fig. 6–F/295/LP1/4.5 and F/295/LP2/4.5 at failure.

Fig. 7–F/215/LP1/4.6 and F/215/LP2/4.6 at failure.

Fig. 8–Flexural failure of F/295/LP1/3.3.

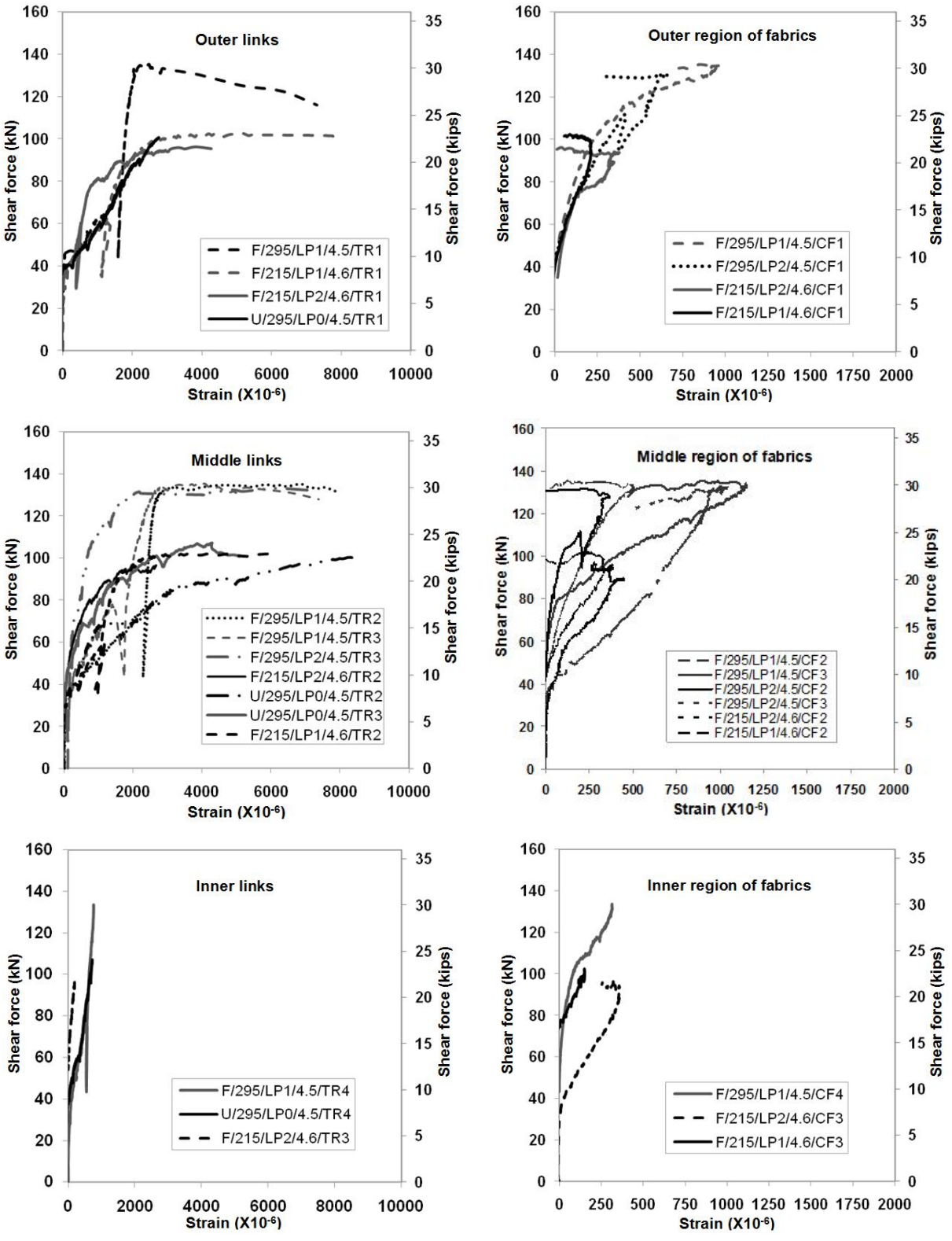

Fig. 9–Shear force versus strain in the internal and external shear reinforcement.